Flutter of Flat Finite Element Panels in a Supersonic Potential Flow

T. Y. Yang*
Purdue University, West Lafayette, Ind.

A finite element formulation and a solution procedure are developed for the flutter analysis of two-dimensional flat panels with one surface exposed to a supersonic potential flow and supported at the leading and trailing edges. The aerodynamic forces due to supersonic flow are obtained from the exact theory for linearized two-dimensional unsteady flow where no limitations on the order of the frequency are imposed. Thus the Mach number need not be limited to beyond approximately 1.6. When using this theory, the aerodynamic matrix becomes location-dependent and must be formulated for each element. This difficulty is overcome by first assembling the element shape functions for the entire structure and then finding the aerodynamic forces and the element aerodynamic matrix by numerical integration. The effects of structural damping and initial inplane tension are included. Examples for finding the panel thickness required to prevent flutter at various Mach numbers are demonstrated and the results are compared with an alternative Galerkin's modal solution as well as experiments.

Nomenclature

$[A]$ = element aerodynamic matrix
c = length of panel chord
E = modulus of elasticity of panel material
F = tension parameter $\bar{F}/c^2\sigma h\omega_1^2$
$\bar{F}$ = initial inplane tensile force per unit width of the panel
$\{F\}$ = vector of forcing function in finite element equations of motion
$f_i(x,y)$ = element shape function associated with ith nodal degree of freedom
g = structural damping coefficient
h = thickness of the panel
$J_i(u)$ = Bessel function of order i of the first kind
k = reduced frequency, $c\omega/2U$
k_1 = stiffness parameter (reduced first natural frequency), $c\omega_1/2U$
ℓ = length of the finite element
M = Mach number
M_i = element bending moment at nodal point i
n = c/ℓ, number of equal-length elements used in the analysis
$\{P\}$ = vector of aerodynamic pressure functions
$\{q\}$ = vector of element nodal displacements
t = time
U = velocity of the supersonic stream
V_i = element transverse force at nodal point i
w = transverse deflection of the panel
w_i = element transverse deflection at nodal point i
x,y = panel middle-plane coordinates with x along the chord and y along the leading edge of the panel
β = $(M^2-1)^{1/2}$
θ_i = element slope at nodal point i
μ = mass ratio between panel and air, $\sigma h/\rho c$
ρ = density in undisturbed supersonic stream
σ = density of panel material
ω = frequency of panel vibration
$\bar{\omega}$ = frequency parameter $2kM^2/\beta^2$
ω_n = nth mode natural frequency
Ω = $(\omega_1/\omega)^2$, in flutter analysis, $\Omega=(\omega_1/\omega)^2(1+ig)$

Received November 15, 1974; revision received February 24, 1975. The author is grateful to H. Lo for fruitful discussions.

Index categories: Aeroelasticity and Hydroelasticity; Structural Dynamic Analysis; Supersonic and Hypersonic Flow.

*Associate Professor, School of Aeronautics and Astronautics. Associate Fellow AIAA.

Introduction

BECAUSE of its versatile applicability, the finite element method appears to be promising for exploring the field of panel flutter. Several studies have begun, with noteworthy success.

In a first attempt, Olson[1] formulated the aerodynamic matrix for a wide-beam finite element and obtained accurate flutter modes and frequencies in the example analysis. Olson[2] later formulated the aerodynamic matrices for two rectangular plate elements (12 and 16 degrees of freedom) and an 18-degree-of-freedom triangular element. The former were applied to rectangular panels and the latter was applied to a delta panel. Flutter modes and frequencies were successfully obtained.

Kariappa and Somashekar[3] formulated the aerodynamic matrix for a 12-degree-of-freedom rectangular element. Kariappa et al.[4] later extended their work[3] to the case of skew panels exposed to the yawed supersonic flow by means of coordinate transformation. The effect of initial tension was included.

In the preceding four references, the linearized flow theory approximated by the first-order frequency of oscillation was used. The Mach number was limited to be beyond 1.6. It thus becomes one of the objectives of this study to include the lower supersonic range in the panel flutter analysis. In this study an exact linearized two-dimensional unsteady flow theory[5] is employed in the finite element formulation. This theory includes the higher order frequencies so that the Mach number can be lower than 1.6.

The aerodynamic force formulated from the exact linearized flow theory involves a complex integration expression which is difficult to be integrated to a closed form and is location-dependent. Location-dependence means that the aerodynamic matrix is different for each finite element at different locations. This is contrary to the conventional concept that every finite element has the same formulation. This paper suggests a procedure in which the shape functions for each element are assembled first for the entire system and then the aerodynamic forces and the element aerodynamic matrix are found by numerical integration. It is, perhaps, this difficulty that hinders the finite element workers from employing the exact linearized flow theory.[1-4]

The exact two-dimensional linearized unsteady theory (strip theory) has been employed by Nelson and Cunningham[6] for flutter analysis of flat panels. They employed the Galerkin's method and assumed the deflection as the summation of natural mode shapes. They also considered the initial tensions by the approximation that the deflection is composed of the summation of natural modes obtained by neglecting the effect of initial tensions.

By the use of the finite element method, however, the effect of initial tensions can be included more exactly. It thus becomes also the objective of this study to include this effect. This aspect is to be elaborated in the subsequent numerical examples.

The three-dimensional linearized unsteady aerodynamic theory has also been employed[7,8] for panel-flutter problems. Since the aerodynamic force is in a form similar to that for the presently used two-dimensional theory, the present development should be basic enough to be extended to include three-dimensional theory. The present examples only emphasize the two-dimensional theory.

Stiffness Equations of Motion

The stiffness equations of motion for a plate finite element under the effect of stiffness, initial inplane force, inertia, structural damping, and aerodynamic force may be written in a matrix form as

$$[K]\ \{q\}+[N]\ \{q\}+[M]\ \{\ddot{q}\}+[A]\ \{q\}=\{F\} \tag{1}$$

The stiffness matrix $[K]$, incremental stiffness matrix $[N]$, and mass matrix $[M]$ have been well developed for almost every plate and shell finite element available. Only the aerodynamic matrix $[A]$ remains to be developed.

a) Formulation Method

In this study, the transverse displacement and the aerodynamic pressure may be assumed, respectively, as

$$\bar{w}(x,y,t)=w(x,y)e^{i\omega t};\ \bar{p}(x,y,t)=p(x,y)e^{i\omega t} \tag{2}$$

The aerodynamic matrix may be derived from the principle of virtual work. The strain energy due to the aerodynamic pressure $p(x,y)$ and the displacement $w(x,y)$ is

$$W=\tfrac{1}{2}\int\int w(x,y)\ p\ (x,y)\ dA \tag{3}$$

The deflection function for a particular element being considered is usually assumed in the form that

$$w(x,y)=\sum_{i=1}^{N} f_i(x,y)\ q_i=\{f\}^T\{q\} \tag{4}$$

where $f_i(x,y)$ is the shape function corresponding to the nodal degree of freedom q_i and N is the total number of degrees of freedom assumed for the element.

The functions for aerodynamic pressure may be assumed, similar to Eq. (4), as

$$p(x,y)=\sum_{i=1}^{N} P_i(x,y)\ q_i=\{P\}^T\{q\} \tag{5}$$

where $P_i(x,y)$ is the pressure function associated with the shape function f_i as well as the nodal degree of freedom q_i.

Substituting Eqs. (4) and (5) into Eq. (3), the strain energy expression becomes

$$W=\tfrac{1}{2}\ \{q\}^T[A]\ \{q\} \tag{6}$$

with

$$[A]=\int\int \{f\}\ \{P\}^T dA \tag{7}$$

By the interpretation of the principle of virtual work, Eq. (7) yields the desired aerodynamic matrix for the particular element being considered.

b) Aerodynamic Pressure

The aerodynamic pressure arises from the vibration of the plate. This pressure is obtained from the exact theory for linearized two-dimensional unsteady supersonic flow (strip theory)

$$\bar{p}(x,t)=\rho[\partial\phi/\partial t+(U/c)\ \partial\phi/\partial x] \tag{8}$$

where the velocity potential for the flow is

$$\phi=\frac{c\,e^{i\omega t}}{\beta}\int_0^x [i\omega w(\xi)+\frac{U}{c}\frac{\mathrm{d}w}{\mathrm{d}\xi}]$$

$$\times e^{-i\bar{\omega}(x-\xi)}J_0[\frac{\bar{\omega}}{M}(x-\xi)\ \mathrm{d}\xi \tag{9}$$

c) Aerodynamic Pressure Function P_i

The aerodynamic pressure function P_i associated with the ith shape function f_i can be obtained from Eqs. (8) and (9) with deflection w replaced by f_i,

$$P_i(x)=\frac{\rho c\omega^2}{\beta}\left\{\int_0^x [-f_i(\xi)+\frac{i}{2k}\frac{\mathrm{d}f_i}{\mathrm{d}\xi}]\right.$$

$$\times e^{-i\bar{\omega}(x-\xi)}J_0[\frac{\bar{\omega}}{M}(x-\xi)]\mathrm{d}\xi$$

$$-\frac{i}{2k}\frac{\mathrm{d}}{\mathrm{d}x}\int_0^x [-f_i(\xi)+\frac{i}{2k}\frac{\mathrm{d}f_i}{\mathrm{d}\xi}]$$

$$\left.\times e^{-i\bar{\omega}(x-\xi)}J_0[\frac{\bar{\omega}}{M}(x-\xi)]\ \mathrm{d}\xi\right\} \tag{10}$$

Upon integration by parts, Eq. (10) is reduced to

$$P_i(x)=\frac{\rho c\omega^2}{\beta}\ [\frac{1}{4k^2}f_i'(x)+\frac{i}{2k}\frac{M^2-2}{\beta^2}f_i(x)$$

$$+\int_0^x f_i(\xi)L\ (x-\xi)\mathrm{d}\xi] \tag{11}$$

where

$$L(\eta)=\{-((M^2+2)/2\beta^4)J_0[(\bar{\omega}/M/\eta)]$$

$$+i(2M/\beta^4)J_1[(\bar{\omega}/M/\eta)]$$

$$+(M^2/2\beta^4)J_2[(\bar{\omega}/M/\eta)]\}e^{-i\bar{\omega}\eta} \tag{12}$$

It is seen in Eq. (11) that the first, second, and third terms are the zero-, first-, and higher-order terms of frequency, respectively.

If the Mach number is greater than approximately 1.6, the effect of the third term in Eq. (11) is negligible. This simplification has been assumed by the previous finite element workers.[1-4] The inclusion of the higher-order frequency terms causes much complexity in the formulation of an aerodynamic matrix. The integration of the variable ξ has to be started from the leading edge of the whole panel to x instead of from the leading edge of a local finite element within which the pressure function $P_i(x)$ is sought. The integration is affected by the location of the finite element.

Because the closed form expression for the third term in Eq. (11) is not obtainable and that the aerodynamic pressure func-

tion is dependent on the location of each finite element, a numerical integration for the formulation of the aerodynamic matrix for each element is suggested.

d) Formulation for a Simple Plate Finite Element

The simplest plate finite element that can be chosen to demonstrate the present formulation procedure is a rectangular plate element that has the same stiffness matrix as an elementary beam element with the bending rigidity EI replaced by $D=Eh^3/12(1-\nu^2)$.

After a careful dimensionalization and derivation, the equations of motion for this element take the form that

$$\begin{Bmatrix} V_1 \\ M_1/l \\ V_2 \\ M_2/l \end{Bmatrix} = \left\{ \Omega \begin{bmatrix} \mu n^5/k_1^4 \begin{bmatrix} 12 & & & \\ 6 & 4 & & \\ -12 & -6 & 12 & \\ 6 & 2 & -6 & 4 \end{bmatrix} \\ +F\mu n^3/10 \begin{bmatrix} 12 & & & \\ 1 & 4/3 & & \\ -12 & -1 & 12 & \\ 1 & -1/3 & -1 & 4/3 \end{bmatrix} \end{bmatrix} - \begin{bmatrix} n\mu/420 \begin{bmatrix} 156 & & & \\ 22 & 4 & & \\ 54 & 13 & 156 & \\ -13 & -3 & -22 & 4 \end{bmatrix} \\ -1/\rho c\omega^2 [A] \end{bmatrix} \right\} \begin{Bmatrix} w_1 \\ \theta_1 \\ w_2 \\ \theta_2 \end{Bmatrix} \tag{13}$$

where matrix $[A]$ is defined by Eq. (7). Equation (13) has been written in symbolic form as Eq. (1).

The element deflection function is generalized to suit the assemblage and numerical integration. For the mth element from the leading edge of the panel, it is in the form that

$$w(\eta) = f_1(\eta)\ w_m + f_2(\eta)\ (l\theta_m) + f_3(\eta)\ w_{m+1} + f_4(\eta)\ (l\theta_{m+1}) \tag{14}$$

with

$$f_1(\eta) = 1 + 2(\eta - m + 1)^3 - 3(\eta - m + 1)^2 \tag{15a}$$

$$f_2(\eta) = (\eta - m + 1) - 2(\eta - m + 1)^2 + (\eta - m + 1)^3 \tag{15b}$$

$$f_3(\eta) = 3(\eta - m + 1)^2 - 2(\eta - m + 1)^3 \tag{15c}$$

$$f_4(\eta) = (\eta - m + 1)^3 - (\eta - m + 1)^2 \tag{15d}$$

where the dimensionless variable η varies from the integer value of $m-1$ to m.

The numerical integration is based on the trapezoidal rule. Each element is broken down into a certain number of segments. The aerodynamic pressure function at a distance x from the leading edge of the whole panel is obtained by

$$P_i(x) = \frac{\rho c\omega^2}{\beta} \left\{ \frac{1}{4k^2} f_i'(x) + \frac{i}{2k} \frac{M^2-2}{\beta^2} f_i(x) + \tfrac{1}{2} \sum_{k=1}^{N} [f_i(\xi_k) L(x-\xi_k) + f_i(\xi_{k+1}) L(x-\xi_{k+1})]\Delta\xi_k \right\} \tag{16}$$

where $\Delta\xi_k = \xi_{k+1} - \xi_k$ and N is the number of segments broken down within the distance x. Since the shape function $f_i(\xi)$ is associated with the ith degree of freedom which is shared by the neighboring elements, it is important that the shape functions for each element be assembled for each common nodal degree of freedom before application of Eq. (16).

Once the aerodynamic pressure functions $P_i(x)$ are obtained for every station in a finite element, the coefficient in the ith row and the jth column of the aerodynamic matrix $[A]$ is obtained from Eq. (7) as

$$A_{ij} = \tfrac{1}{2} \sum_{k=1}^{M} [P_i(x_k) f_j(x_k) + P_i(x_{k+1})\, f_j(x_{k+1})]\Delta x_k \tag{17}$$

where $\Delta x_k = x_{k+1} - x_k$; x_1 and x_{M+1} are the x-coordinates of the first and the last nodal edges of the element, respectively; and N is the numer of segments broken down within the element.

Numerical Procedure

The condition of flutter is determined from the nontrivial solution of the equations of motion for the panel system. The flutter boundary for each mode is determined by searching for the complex eigenvalue Ω, defined as $(\omega_1/\omega)^2(1+ig)$, for which the structural damping coefficient g vanishes. For a given problem, the initial inplane tensile force F, the Mach number M, and the boundary conditions are first defined. A specific value of the reduced frequency k is then assumed. By varying the air-panel mass ratio $1/\mu$, the corresponding complex eigenvalues Ω are found. If the g values obtained vary from positive to negative, the corresponding $1/\mu$ values travel from the unstable region to the stable region and vice versa.

Evaluation and Application

The examples chosen are the rectangular flat panels with the leading and trailing edges clamped while the other two edges are free. One surface of the panels is exposed to a supersonic potential flow with Mach number of 1.3, $\sqrt{2}$, 1.56, 2.0, and 3.0, respectively. The flutter boundaries are obtained for each Mach number by the use of four finite elements. Each finite element is broken down into 10 segments for numerical integration. The initial inplane tensile force parameters F with values of 0.1, 0.5, and 1.0 are then included to obtain various results. Strong beneficial effect due to the initial tension is indicated.

a) Mach Number of 1.3

The results for the flutter boundaries for a flow of Mach number 1.3 are shown in Fig. 1 for the first two modes. The mode shapes for the real parts of the complex eigenvectors are also shown in Fig. 1. The ordinate is the air-panel mass ratio $1/\mu = \rho c/\sigma h$. The abscissa is the stiffness parameter $2k_1 = c\omega_1/U$ where ω_1 is the first natural frequency of the plate vibrating in vacuum. Some selective values of the reduced frequency $k = c\omega/2U$ are marked along the curves. An alternative solution by the use of Galerkin's method with the deflection approximated by a summation of four natural modes is available for comparison.[6] The agreement is good. In Fig. 1, the region on the right of the first-mode boundary is

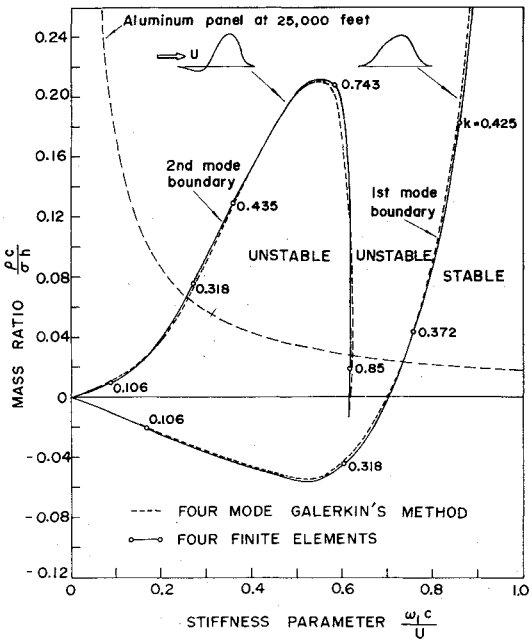

Fig. 1 Flutter boundaries for clamped-edge panels with $M = 1.3$.

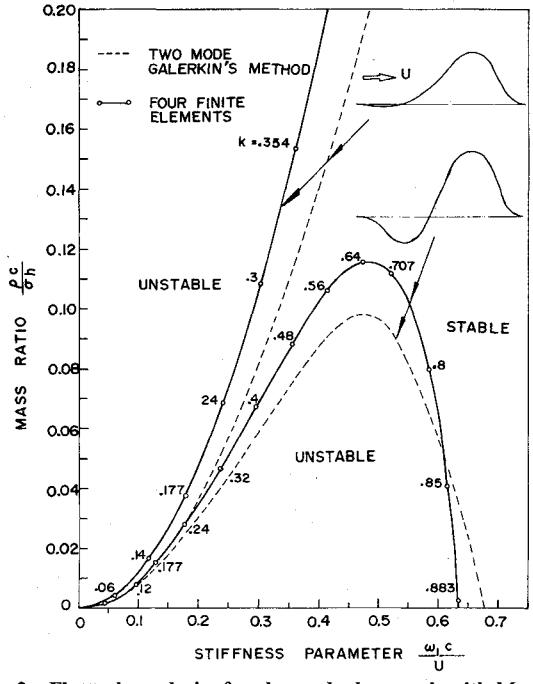

Fig. 2 Flutter boundaries for clamped-edge panels with $M = \sqrt{2}$.

unstable and the other side is stable. For the second mode, the region above the curve is stable and the region below is unstable.

The product of the two nondimensional quantities $1/\mu$ and $2k$ results in an expression involving parameters of ρ, σ, E, ν, and M. If the values for these parameters are specified, the product of $1/\mu$ and $2k_1$ can be plotted as a parabola in the $1/\mu$ vs $2k_1$ plane. For instance, an aluminum panel at an altitude of 25,000 ft can be represented by the dashed hyperbola shown in Fig. 1. The intersection of the hyperbola with the first-mode flutter boundary gives $1/\mu$ a value of 0.0231 and h/c a value of 0.0085 that define the state of neutral stability. A thicker panel will be stable and a thinner panel will flutter.

It is found that the effect of the structural damping coefficient g moves the first-mode boundary slightly to the left. The damping has, however, a pronounced effect that reduces the second-mode boundary. These results are not shown here. But such effect is presented subsequently for a more representative case, with $M = \sqrt{2}$.

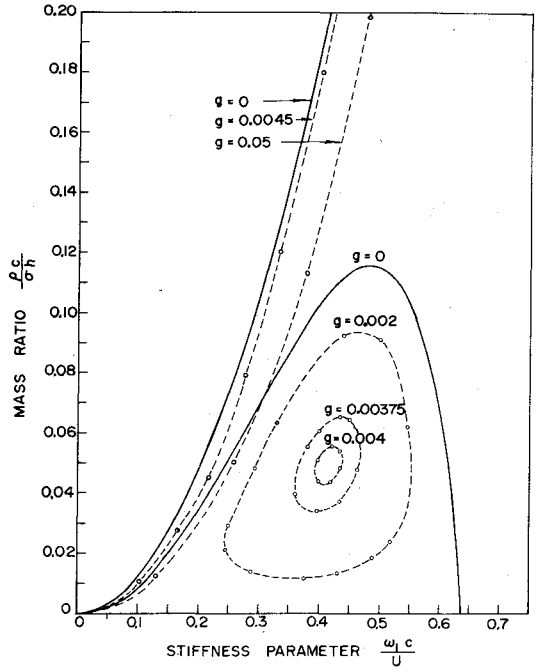

Fig. 3 Flutter boundaries for clamped-edge panels with $M = \sqrt{2}$ for various values of structural damping coefficient g (four finite element solution).

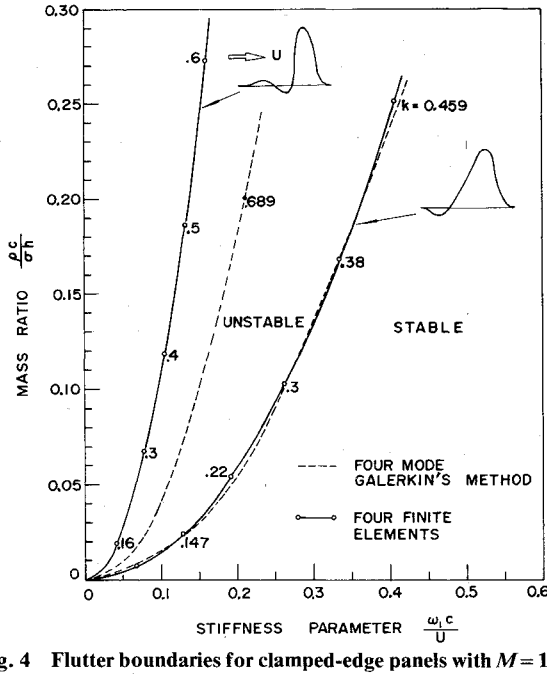

Fig. 4 Flutter boundaries for clamped-edge panels with $M = 1.56$.

b) Mach Number of $\sqrt{2}$

The results for Mach number $\sqrt{2}$ are shown in Fig. 2. A two-mode (two-degree-of-freedom) Galerkin's solution[6] is also shown for comparison. The agreement between the two solutions would be improved considerably if a four-mode analysis were performed by the method of Ref. 6. The upper dashed curve was referred to "loosely" in Ref. 6 as the first-mode boundary and the lower dashed curve as the second-mode boundary. In the present four-finite-element (six-degree-of-freedom) analysis, the mode shapes obtained by plotting the real values of the eigenvectors are shown in Fig. 2 for both boundaries. Although the mode shape for the upper boundary appears to be nearly of the second mode, it may be loosely interpreted as the first mode. The mode shape associated with the lower boundary is clearly of the second mode. From the k values marked along both curves, it can be

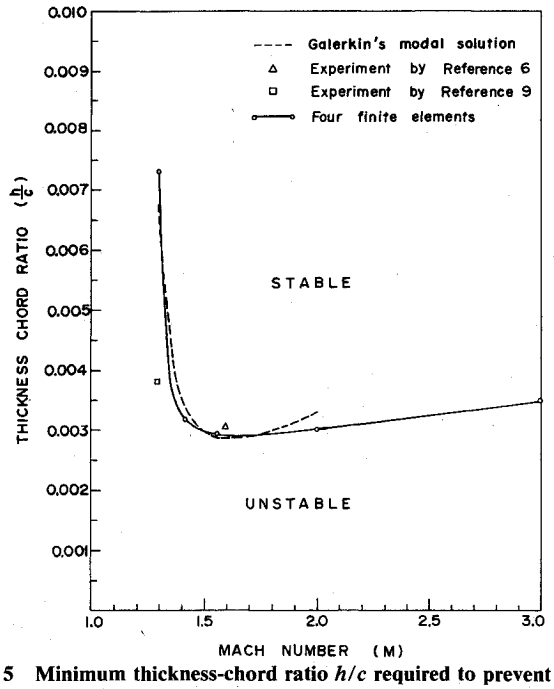

Fig. 5 Minimum thickness-chord ratio h/c required to prevent flutter of aluminum panel at 25,000 feet altitude (with $g = 0.0045$).

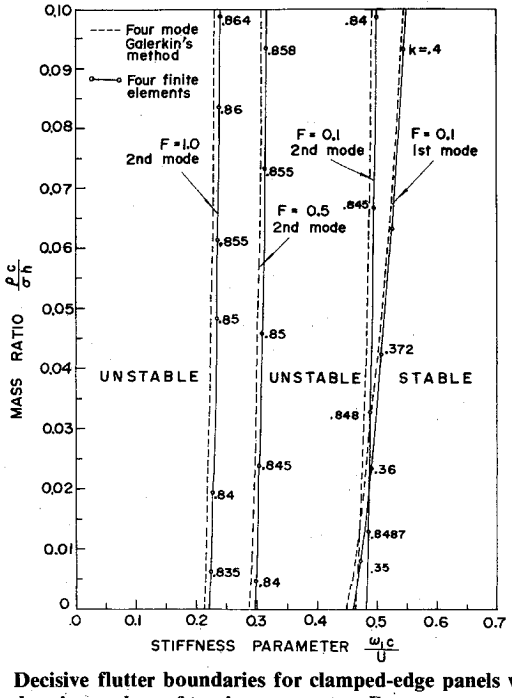

Fig. 6 Decisive flutter boundaries for clamped-edge panels with $M = 1.3$ and various values of tension parameters F.

calculated that the frequencies are approximately $2.7\omega_1$ for the lower boundary and $1.96\omega_1$ for the upper boundary.

Unlike the case of $M = 1.3$, the lower boundary in Fig. 2 has a decisive effect on the panel thickness required to prevent flutter. But it is found that this boundary is considerably reduced for small values of g, as shown in Fig. 3. This boundary virtually vanishes, as g is greater than 0.004. For the upper boundary, the effect of g is small.

c) Mach Numbers of 1.56, 2, and 3

The results for flutter boundaries for Mach number of 1.56 are shown in Fig. 4. The mode shapes for the real parts of the eigenvectors are also shown. The results from a four-mode Galerkin's method[6] are shown for comparison. The agreement for the decisive second-mode boundaries between the two solutions is good. The results for flutter boundaries

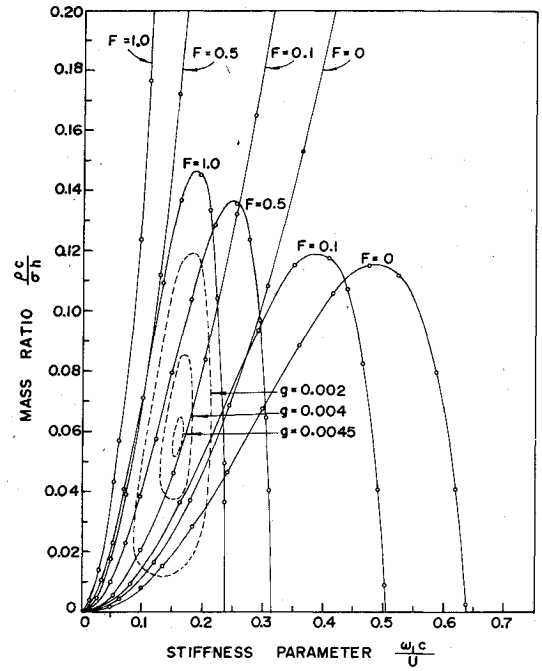

Fig. 7a) Flutter boundaries for clamped-edge panels with $M = \sqrt{2}$ and various values of tension parameter F. b) Second mode flutter boundaries for $F = 1.0$ and various values of damping coefficient g.

for Mach numbers 2 and 3 were obtained but are not shown here. They are similar to, but on the left of, those curves shown in Fig. 4.

d) Variation with Mach Number

It has been indicated in Fig. 2 that for $M = \sqrt{2}$ the second-mode (lower) boundary rather than the first-mode (upper) boundary has a decisive effect in determining the panel thickness required to prevent flutter. It has been indicated in Fig. 3 that, for small damping coefficient g, this decisive boundary shrinks rapidly while the first-mode boundary shifts only slightly. For a value of g slightly greater than 0.004, the second-mode boundary no longer exists. Consequently, the first-mode boundary becomes decisive. A similar phenomenon is found for $M = 1.3$. In that case, the second-mode boundary disappears when g is slightly greater than 0.03.

As an example, an aluminum-alloy panel at an altitude of 25,000 ft is considered. A plot of the minimum thickness-chord ratio required to prevent flutter vs Mach number is shown in Fig. 5. A small g value of 0.0045 is assumed, so that the second-mode boundary for $M = \sqrt{2}$ does not exist. Such damping coefficient slightly affects the first-mode boundaries for $M = 1.3$ and $\sqrt{2}$, but has no effect on the boundaries for $M = 1.56$ and higher.

A similar curve obtained by Nelson and Cunningham[6] is also shown in Fig. 5. They used four-mode Galerkin's analysis for $M = 1.3$ and 1.56 but two-mode analysis for $M = \sqrt{2}$. Two experimental data[6,9] are also shown in the figure.

e) With Initial Inplane Tensile Forces

The effect of initial inplane tensile forces F is first studied for the case of $M = 1.3$. The introduction of such forces has a marked effect that shifts the flutter boundaries toward the left, i.e., decreasing the panel thickness required to prevent flutter. As F increases, the first-mode boundary moves to the left faster than the higher-mode boundaries and thus the higher-mode boundaries become decisive. Figure 6 shows only those decisive flutter boundaries for $M = 1.3$ and $F = 0.1$, 0.5, and 1.0. The results from the four-mode Galerkin's method[6] are also shown. Nelson and Cunningham[6] reported that for $F = 1.0$ the third-mode boundary shifted slightly to the right of

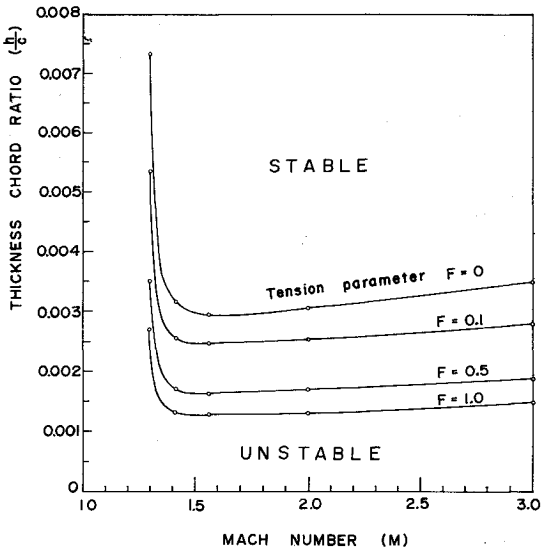

Fig. 8 Minimum thickness-chord ratio h/c required to prevent flutter of aluminum panel at 25,000 feet altitude (with $g=0.0048$ and various values of tension parameter F).

the second-mode boundary. This phenomenon is, however, not found here.

A comparison between the present solution and that from Ref. 6 reveals some discrepancies that have not been noted for the case with no initial tensile force. This may be attributed to the oversimplified manner in which the initial tensions were handled in Ref. 6. For a clamped edge panel, the natural frequencies and mode shapes are affected by the initial tensions. However, in the modal approximation method used by Ref. 6, the mode shapes employed were those obtained by neglecting the effect of initial tensions.

The results for $M=\sqrt{2}$ are shown in Fig. 7. The initial tensions are seen to have a strong influence that pushes both the first, and second-mode flutter boundaries to the left. For the case of $F=1.0$, the effect of damping coefficient g is also shown. The second-mode boundary shrinks rapidly for small-g and disappears for $g=0.0048$. The first-mode boundary remains unchanged for such a small g value. When $F=0.1$ and 0.5, the second-mode boundaries disappear for $g=0.0048$, but the first-mode boundaries shift slightly to the right.

The effects of initial tensions on the decisive flutter boundaries for the cases of $M=1.56$, 2, and 3 have also been studied but not shown here. The results are all similar to those shown in Fig. 6. The initial tensions are found to have an effect that pushes the decisive boundaries to the left. Furthermore, those curves have been found to be unaffected by a small damping coefficient of $g=0.004$.

Finally, an aluminum-alloy panel at an altitude of 25,000 ft under various initial tensions is considered. A small g value of 0.0048 is included so that the second-mode boundary for $M=\sqrt{2}$ does not exist. A plot of the minimum thickness-chord ratio required to prevent flutter vs Mach number is shown in Fig. 8. The minimum panel thicknesses drop considerably as the initial tensions are increased.

Conclusions

When the exact strip theory for the two-dimensional unsteady flow is used, the element aerodynamic matrix becomes location dependent. This paper suggests a procedure first to assumble the element shape functions and then to find the aerodynamic forces at every integration point for the entire structure. By using the shape functions and the aerodynamic forces, the element aerodynamic matrix is found by numerical integration. This procedure is demonstrated by formulating a simple long-plate element and performing examples. The results are found in good agreement with an alternative Galerkin's solution[6] as well as experiments.[6,9]

The present method includes the effect of initial tensions more accurately than does Ref. 6. Examples are performed. The initial tensions are found to have strong beneficial effect against panel flutter. This development may provide a basis for the flutter analysis of more realistic cases. Feasible future work might include panels with finite aspect ratios, an anisotropic panel, elastic restrained edges, and panels buckled due to temperature rises, etc. Alternative solutions for these cases are, in fact, available for comparison.[7,8,10,11]

References

[1] Olson, M. D., "Finite Elements Applied to Panel Flutter," *AIAA Journal*, Vol. 5, Dec. 1967, pp. 2267-2270.

[2] Olson, M. D., "Some Flutter Solutions Using Finite Elements," *AIAA Journal*, Vol. 8, April 1970, pp. 747-752.

[3] Kariappa and Somashekar, B. R., "Application of Matrix Displacement Methods in the Study of Panel Flutter," *AIAA Journal*, Vol. 7, Jan. 1969, pp. 50-53.

[4] Kariappa, Somashekar, B. R. and Shah, C. G., "Discrete Element Approach to Flutter of Skew Panels with In-Plane Forces under Yawed Supersonic Flow," *AIAA Journal*, Vol. 8, Nov. 1970, pp. 2017-2022.

[5] Shen, S. F., "Flutter of a Two-Dimensional Simply Supported Uniform Panel in a Supersonic Stream," ONR Contract N5ori-07833, Aug. 1952, Dept. of Aeronautical Engineering, MIT, Cambridge, Mass.

[6] Nelson, H. C. and Cunningham, H. J., "Theoretical Investigation of Flutter of Two-Dimensional Flat Panels with One Surface Exposed to Supersonic Potential Flow," NACA TR1280, 1956.

[7] Cunningham, H. J., "Flutter Analysis of Flat Rectangular Panels Based on Three-Dimensional Supersonic Unsteady Potential Flow," NASA TR R-256, 1967.

[8] Dowell, E. H. and Voss, H. M., "Theoretical and Experimental Panel Flutter Studies in the Mach-Number Range 1.0 to 5.0," *AIAA Journal*, Vol. 3, Dec. 1965, pp. 2292-2304.

[9] Sylvester, M. A. and Baker, J. E., "Some Experimental Studies of Panel Flutter at Mach Number 1.3," NACA RM L52I16, 1952.

[10] Erickson, L. L., "Supersonic Flutter of Flat Rectangular, Orthotropic Panels Elastically Restrained Against Edge Rotation," NASA TN D-3500, 1966.

[11] Ventres, C. S. and Dowell, E. H., "Comparison of Theory and Experiment for Nonlinear Flutter of Loaded Plates," *AIAA Journal*, Vol. 8, Nov. 1970, pp. 2022-2030.